Chemical Engineering Journal 351 (2018) 1137–1146

Contents lists available at ScienceDirect

Chemical Engineering Journal

journal homepage: www.elsevier.com/locate/cej

Degradation of acetamiprid in UV/H_2O_2 and UV/persulfate systems: A comparative study

Liwei Chen, Tianming Cai, Chuan Cheng, Zhuang Xiong, Dahu Ding*

College of Resources and Environmental Sciences, Nanjing Agricultural University, Nanjing 210095, China

HIGHLIGHTS

- UV/PS process was much more effective than the UV/H_2O_2 process in degrading ACE.
- The TOC removal rate achieved 50% and 26.6% for the UV/PS and UV/H_2O_2, respectively.
- The degradation was greatly inhibited in secondary effluent of wastewater treatment facility.
- Second-order rate constants of ACE with $^{\cdot}OH$ and $SO_4^{\cdot -}$ were derived.

ARTICLE INFO

Keywords:
Sulfate radical
Hydroxyl radical
Second order rate constant
Secondary effluent
Advanced oxidation

ABSTRACT

Acetamiprid (ACE) was degraded by using ultraviolet (UV) irradiation and UV based advanced oxidation processes (AOPs) including UV/hydrogen peroxide (UV/H_2O_2) and UV/potassium persulfate (UV/PS). Among them, UV/PS process exhibited the best performance for the elimination of ACE and reduction of total organic carbon (TOC). The degradation kinetics was comprehensively compared in terms of dose of oxidants, solution pH, and water matrix species. A linear relationship was tentatively developed between the [Oxidant]/[ACE] ratio and the pseudo-first-order kinetic rate constant (k). The degradation was significantly inhibited at basic conditions no matter for UV/H_2O_2 process or UV/PS process. The effects induced by the water matrix species including inorganic anions and natural organic matter (NOM) were also non-negligible. For UV/PS process, both $SO_4^{\cdot -}$ and $HO^{\cdot}$ contributed to the ACE degradation, whereas only $HO^{\cdot}$ participated in the degradation in the UV/H_2O_2 process. The corresponding second-order rate constants of ACE with $HO^{\cdot}$ and $SO_4^{\cdot -}$ were determined to be 7.59×10^8 and $3.68 \times 10^8\ M^{-1}\,s^{-1}$, respectively. Due to the different active radical species, different degradation products were detected through the HPLC-MS analysis. This work would be meaningful for the remediation of ACE from water by AOPs.

1. Introduction

Acetamiprid (ACE), chemically known as N-[(6-chloro-3-pyridyl) methyl]-N'- cyano-N-methyl-acetamidine, is a typical neonicotinoid insecticide. According to its relatively low acute and chronic mammalian toxicity, ACE exhibits broader applications than conventional insecticides which have caused severe environmental pollution and pesticide-resistance issues [1]. As a consequence, ACE has been intensively detected in different environmental media, such as soil and vegetables [2–4]. The maximum residue limit (MRL) for ACE in vegetables and fruits is strictly regulated ($< 5\,\mu g\,g^{-1}$ in Japan and $< 3\,\mu g\,g^{-1}$ in United States, respectively) [5,6]. However, with high water solubility ($4250\,mg\,L^{-1}$), ACE can be readily washed out from the soil and invade the aquatic environment. Noteworthily, due to its bio-refractory and recalcitrant nature, ACE cannot be effectively removed by conventional biological wastewater treatment processes [7]. It has been detected in the secondary effluents at concentrations ranging from $50\,ng\,L^{-1}$ [8] to $16\,\mu g\,L^{-1}$ [9]. The presence of ACE in the environment can pose potential risks to human health and aquatic systems. For example, the European Food Safety Authority (EFSA) recently delivered a Scientific Opinion claiming that chronic exposure to ACE could affect neural development and function in humans [10]. Recently, some other adverse effects on human health were associated with the chronic exposure to ACE, including memory loss and finger tremors [11]. In addition to human beings, ACE would pose negative effects on other species such as aquatic and soil microorganisms, as well as beneficial insects [12]. Therefore, it is very desirable to develop effective methods to remove the residual ACE in water [13].

* Corresponding author at: 1 Weigang, Xuanwu District, Nanjing 210095, China.
E-mail address: ddh@njau.edu.cn (D. Ding).

https://doi.org/10.1016/j.cej.2018.06.107
Received 15 March 2018; Received in revised form 5 June 2018; Accepted 16 June 2018
Available online 27 June 2018
1385-8947/

Biodegradation is recognized as an economically competitive method for the elimination of organic pollutants from environmental media. For instance, Yang et al. [14] successfully isolated an ACE-degradable strain D-2 from a wastewater treatment pool located in an ACE-manufacturing factory. However, the degradation process was extremely time-consuming (~72 h) and therefore significantly limited its application. Moreover, the metabolism of ACE by pure strain was regulated by specific functional genes, which possessed high selectivity towards target organic compounds. Consequently, the ACE was hardly to be completely mineralized to the end products, i.e. CO_2 and H_2O [15]. On the other hand, the chemical methods especially advanced oxidation processes (AOPs) could remarkably reduce the reaction time and more easily achieve the mineralization [16,17]. Through generation of strong oxidative radical species (hydroxyl radical, sulfate radical, and etc.), various organic pollutants could be completely decomposed within several hours [18]. For instance, Cao et al. [19] reported the photocatalytic degradation of ACE by using the Ag doped TiO_2 nanoparticles. The half-live of the degradation process was no longer than 20 min. Moreover, the degradation rate could be further enhanced significantly by adding the electron acceptors (H_2O_2, $KBrO_3$, $K_2S_2O_8$) [20]. Carra et al. [21] investigated the degradation of ACE in an UVC-LED enhanced photo-Fenton process. The ACE at a concentration of 100 μg L^{-1} in synthetic secondary effluent could be removed within 20 min by adding (1 + 1 + 1) mg L^{-1} Fe^{2+} (sequential iron dosage) and 12 mg L^{-1} H_2O_2. They also compared the performance of various photo-Fenton processes (UV/TiO_2, UV/H_2O_2, and UV/persulfate (UV/PS)) for the abatement of ACE from water [22]. Among them, the UV/H_2O_2 and UV/PS processes exhibited great potential for the removal of ACE from deionized water and synthetic secondary treated wastewater. However, some important points need to be further elucidated. For example, the degradation behavior of ACE by the AOPs is not comparatively investigated. The underlying degradation mechanism especially in the UV/PS process has yet been clearly revealed. The effective degradation of ACE in natural waters deserves to be further investigated.

To fulfill the abovementioned gaps, the ACE degradation by UV/H_2O_2 and UV/PS processes was particularly focused in this study. The influences of environmental conditions (solution pH, inorganic anions, natural organic materials (NOM)) on the degradation processes were systematically investigated. Specifically, the degradation behaviors in natural waters (river water, lake water, and treated wastewater) were tentatively studied for the first time. Moreover, the degrees of mineralization and degradation products were detected, respectively. Finally, the contributions of the reactive oxidative species were distinguished.

2. Materials and methods

2.1. Materials

High purity ACE (99%) was obtained from Jiangsu Changqing Agrochemical Co. Ltd., China. The basic information of ACE was listed in Table 1. Reagent-grade hydrogen peroxide (35 wt%), potassium persulfate (99.9%) were purchased from Aladdin, China. All the other reagents used in this study were obtained from Sinopharm, China or Aladdin, China and used without further purification. Solutions used in the experiments were prepared with deionized water from a water purification system (EPED-S2).

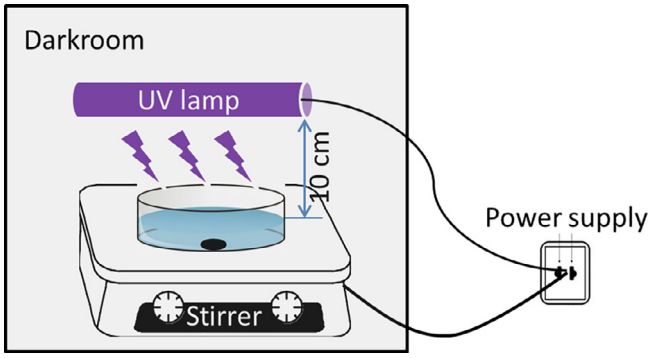

Scheme 1. The sketch diagram of the UV irradiation apparatus applied in this study.

The river water, lake water, and secondary effluent (SE) of wastewater were collected from Yangtze river (YR), Taihu lake (TL), and wastewater treatment facility located in a local insecticide factory, respectively. The fresh water samples were filtered with qualitative filter paper (Whatman, GE) upon arrival and stored under 4 °C in a refrigerator.

2.2. Experimental procedure

As given in Scheme 1, the degradation experiments were conducted in an air-conditioned darkroom (~25 °C). A glass dish served as the reactor was placed under a Philips UV lamp (851 mm in length, 55 W, emission at 253.7 nm). The distance between the lamps and the liquid level was approximately 10 cm. The thickness of the ACE solution (50 mL) was around 1 cm to ensure the radiation intensity in the mixture. Due to the low power of the lamp and the distance between lamp and solution, the temperature of reaction mixture was not significantly changed during irradiation process. Therefore, no cooling system was applied in this study and the water loss through evaporation was negligible. The ACE solution was magnetically agitated (~50 rpm) to maintain the homogeneity throughout the reaction. The solution pH was adjusted by using 0.1 M H_2SO_4 or NaOH. Water samples were collected at regular time intervals and quenched with equal volume of methanol immediately to stop the reactions. Each experiment was conducted for at least 2 times and the average and standard deviations were reported. The effects of inorganic anions and organic matter on the degradation process were also investigated respectively.

For the radical-quenching studies, excess methanol and *tert*-butanol were added into the solution prior to the oxidants. According to the distinct reaction rate constants, the *tert*-butanol could consume HO· prior to the organic pollutants while methanol could scavenge HO· and $SO_4^{\cdot -}$ effectively [23,24].

For the determination of degradation products, the treated ACE solution was concentrated with a solid phase extraction cartridge (WAT106202, Waters Oasis). The HLB cartridge was pre-activated prior to the use with 5 mL methanol and 5 mL Milli-Q water, respectively. The final extracted sample was obtained by eluting with 4 mL methanol

Table 1
The basic information of the insecticide acetamiprid.

Molecule	MW (g mol^{-1})	Structure	p*Ka*	Water solubility (mg L^{-1})	Logk_{ow}	Henry's law constant (atm m^3 mol^{-1})	Vapor pressure (mm Hg)
$C_{10}H_{11}ClN_4$	222.676	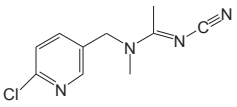	0.7	4250	0.8	6.9×10^{-8}	4.4×10^{-5}

Data source: PubChem, https://pubchem.ncbi.nlm.nih.gov/compound/213021.

(2 mL × twice).

2.3. Kinetic analysis

The degradation of organic compounds by AOPs usually follows the pseudo-first-order kinetics (especially for the initial period) [25–29]. The derived apparent rate constant (k) could indicate the rate of the whole reaction to some extent. Therefore, the pseudo-first-order kinetic model shown in Eq. (1) was adopted to mimic the degradation kinetics in this study.

$$\ln\left(\frac{C_t}{C_0}\right) = -kt \quad (1)$$

where C_0 is initial concentration of ACE, C_t is concentration of ACE at time t, k is the apparent pseudo-first order constant. By plotting ln (C_t/C_0) versus t, k can be graphically calculated.

2.4. Determination of the second-order rate constants

Competition kinetic approaches were applied to determine the second-order rate constants of HO· and $SO_4^{\cdot -}$ with ACE, using *para*-chlorobenzoic acid (pCBA) and *meta*-toluic acid (mTA) as competitors [24,30]. Experiments were conducted in phosphate buffer (PB) at pH 7. Concentrations of ACE and competitors were 90 μM and 100 μM, respectively. The concentrations of H_2O_2 and PS were 12 mM and 2 mM, respectively. Noting that, although $SO_4^{\cdot -}$ can react with OH^- to generate HO· in UV/PS system, the reaction could be neglected at pH 7 [31]. Detailed information for competition kinetic methods was shown in Supporting Information Text S1.

2.5. Analytical methods

The concentration of ACE was measured using a high performance liquid chromatograph (HPLC, FL 2200) equipped with a C 18 column. Aliquots of 20 μL were injected manually through an injection loop. Column temperature was held at 25 °C, mobile phase was consisted of acetonitrile (35%) and water (65%), and the flow rate was 0.8 mL min^{-1}. Acetamiprid was monitored at 248 nm (ACE absorption maximum) with the retention time being 8.1 min. The UV spectrum of ACE solution was recorded with a Cary 50 spectrophotometer (VARIAN). TOC of the water samples were determined by a Shimadzu TOC VCSH analyzer with an ASI-V auto sampler. COD_{Cr} and total salinity of the real waters were measured according to the standard method [32]. Inorganic anions were detected by using an ion chromatography (Thermo ICS 900). pH value was determined with a pH meter (Leici).

The Agilent 1200 series HPLC coupled with an Agilent G6410B triple quadrupole (QQQ) mass spectrometer (Agilent Technologies, USA) was adopted for the detection of degradation products. The detailed operation conditions of the HPLC-MS were given in Supporting Information Text S2.

3. Results and discussion

3.1. Degradation of ACE in deionized water

Fig. 1 shows the overall degradation performance of ACE by UV, UV/H_2O_2 and UV/PS processes. Due to the refractory property, the ACE could not be decomposed effectively with only chemical oxidants (H_2O_2 or PS). Accordingly, no more than 15% of the degradation rate was observed within 60 min. On the other hand, near 30% ACE was reduced with the direct UV irradiation. This reduction was probably attributed to the direct photolysis of organic compounds [33]. The direct photolysis was highly dependent on the decadic molar absorption coefficient of the compound at a certain wavelength [34]. The results meant that ACE could absorb the photons in UV radiation with wavelength at 254 nm, agreeing well with the UV spectrum of ACE solution which showed a remarkable absorption peak at 220–260 nm (Fig. S1). Kim and Tanaka [35] investigated the degradation of over 30 kinds of pharmaceutical and personal care products (PPCPs) with UVC irradiation and classified them into easily-degrading PPCPs ($k \geq 2.6 \times 10^{-3}\ s^{-1}$) and slowly-degrading PPCPs ($k < 6.4 \times 10^{-4}\ s^{-1}$). In this case, the k of ACE during the UV treatment was around $8.3 \times 10^{-5}\ s^{-1}$, belonging to the slowly-degrading PPCP.

With the UV radiation, the chemical oxidants such as H_2O_2 and PS can be transferred into powerful free radicals through the following reactions [36,37].

$$H_2O_2 + h\nu \rightarrow 2HO^{\cdot} \quad (2)$$

$$S_2O_8^{2-} + hv \rightarrow 2SO_4^{\cdot -} \quad (3)$$

As a result, the UV based AOPs (UV/PS and UV/H_2O_2) possessed significantly enhanced degradation performance (Fig. 1). Over 60% of ACE was removed from the aqueous solution within 60 min by the UV/H_2O_2 process. Meanwhile, almost complete degradation was achieved by the UV/PS process. The remarkably accelerated degradation processes revealed that there should be a synergistic effect between UV radiation and chemical oxidants. Moreover, the higher k value clearly indicated that the UV/PS process was much more effective than the UV/H_2O_2 process in degrading ACE (Fig. S2). It was also the case for the degradation of antiepileptic drug carbamazepine and azo dye [22,38,39]. This was probably due to that PS was more photosensitive than H_2O_2 [40], resulting a higher radical production yield in the UV/PS process [41]. However, it was not the case for the degradation of antipyrine [42]. The degradation rate of antipyrine followed the order of UV/H_2O_2 > UV/PS. The probable reason was that the reactivity (second-order rate constant) of organic compounds with different radical species was different [27].

To verify this hypothesis and identify the contributions of HO· and $SO_4^{\cdot -}$ in the degradation process, the corresponding second-order rate constants were determined by competition kinetics. The derived second-order rate constants of ACE with HO· and $SO_4^{\cdot -}$ were calculated to be 7.59×10^8 and $3.68 \times 10^8\ M^{-1}\ s^{-1}$, respectively (Fig. S3). Therefore, the distinct reactivity of ACE with different radical species could probably be ruled out because of the comparable second-order rate constant.

3.2. Effect of oxidant dosage

Fig. 2 depicts the degradation profiles of ACE in UV/H_2O_2 and UV/PS processes with different oxidant dosage (expressed in terms of [Oxidant]/[ACE] ratio). Generally, the degradation rate would be proportional to the amount of radicals at the low concentrations of chemical oxidants. However, the excess oxidants would inhibit the degradation process due to the self-scavenging effect [29,36]. In this case, the degradation rate constant increased with the [H_2O_2]/[ACE] ratio, indicating the concentration of H_2O_2 was below the inhibition point [38]. On the other hand, the rate constant was nearly unchanged when the [PS]/[ACE] ratio is higher than 20. Moreover, the degradation rate constants exhibited a linear relationship with the oxidant dosage (UV/H_2O_2: $k = 0.00081 \times ([H_2O_2]/[ACE]) + 0.00352$ ($[H_2O_2]/[ACE] < 30$) and $k = 0.00019 \times ([H_2O_2]/[ACE]) + 0.0314$ ($[H_2O_2]/[ACE] > 60$); UV/PS: $k = 0.0049 \times ([PS]/[ACE]) - 0.028$, ($[PS]/[ACE] < 20$)) [42,43]. As shown in Fig. 2C, the slope was significantly reduced when the [H_2O_2]/[ACE] ratio was higher than 60, meaning the increase rate of k reduced. Similarly, the slope was absolutely near 0 when the [PS]/[ACE] ratio was higher than 20. This was probably due to the self-scavenging effect. Similar phenomenon was also reported in previous study [44].

Noting that, the ACE could not be efficiently removed in the UV/

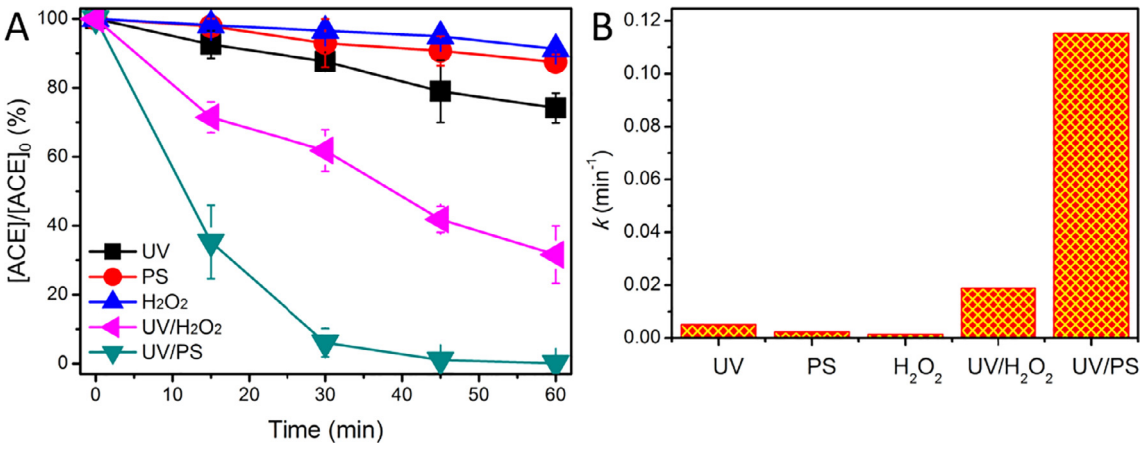

Fig. 1. The overall degradation performance of ACE in UV, PS, H_2O_2, UV/PS, and UV/H_2O_2 systems (A), and the corresponding pseudo-first-order kinetic rate constant (B). ([ACE] = 90 μM, [H_2O_2] = [$K_2S_2O_8$] = 1.5 mM, pH = 7, T = 25 °C).

H_2O_2 system unless the [H_2O_2]/[ACE] was higher than 65. Therefore, we conducted the following experiments with the [H_2O_2]/[ACE] was 130 ([H_2O_2] = 11.8 mM, [ACE] = 90 μM).

3.3. Effect of solution pH

Fig. 3 presents the degradation of ACE at different pH values. The results clearly indicated that both of the processes were highly dependent on the solution pH. As well known, the solution pH played two important roles during the degradation process. Firstly, the active oxidation species in the solution was greatly influenced by the solution pH [45]. Secondly, the organic compounds would be transferred into different forms according to their specific p*K*a(s) under varied solution pHs, leading to the distinct reactivity towards radical species [46]. For this study, the p*K*a of ACE was 0.7, far below the studied pH values. The difference of degradation rate brought by the different dissociated forms of ACE could be therefore excluded. Besides, the reduction of ACE resulted from the hydrolysis at different pH values could be ignored because the hydrolysis process is rather time-consuming (took for several days) [7].

For the UV/H_2O_2 process, the degradation was significantly inhibited under basic conditions. This was probably due to the reduction of oxidation power of HO· because the redox potential $E_{HO\cdot,H2O}$ decreased from 2.62 to 2.15 V with pH increasing from 3 to 11 (derived

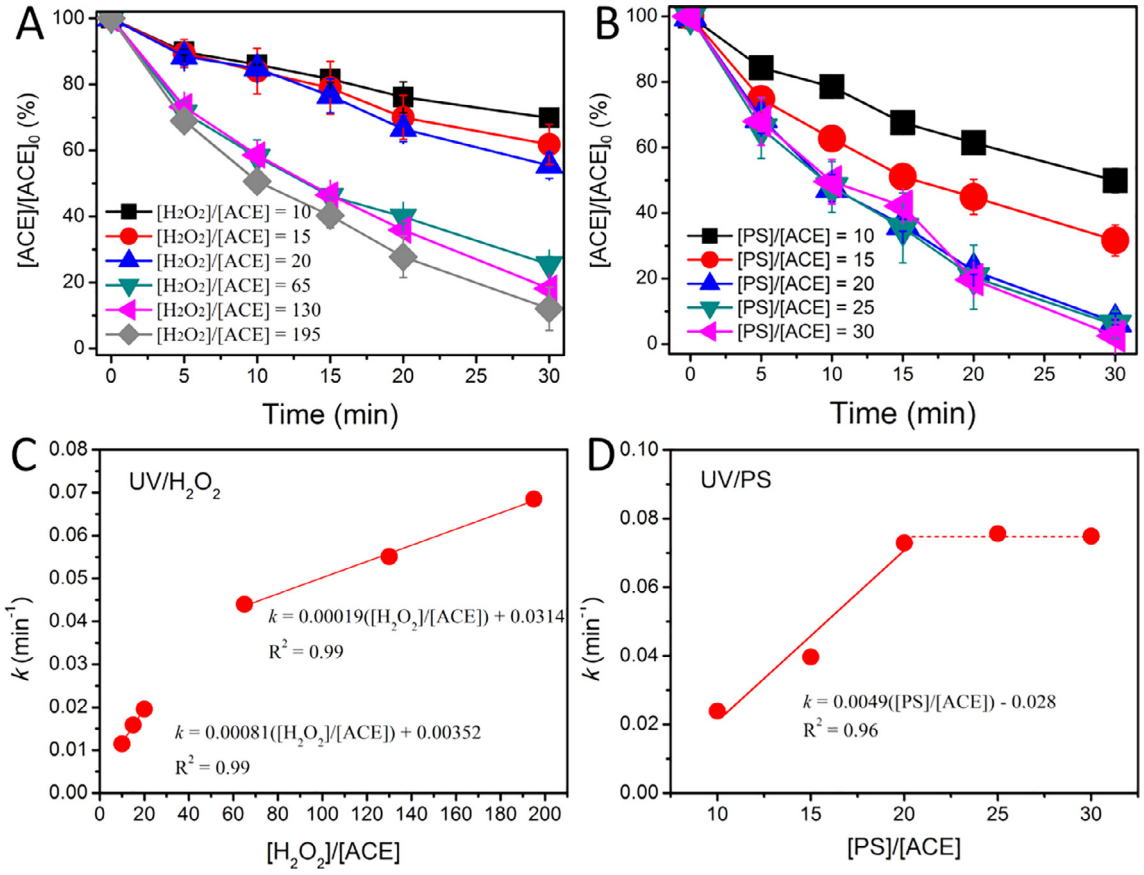

Fig. 2. The degradation of ACE in UV/H_2O_2 (A) and UV/PS (B) systems with different [Oxidant]/[ACE] ratios. ([ACE] = 90 μM, pH = 7, T = 25 °C).

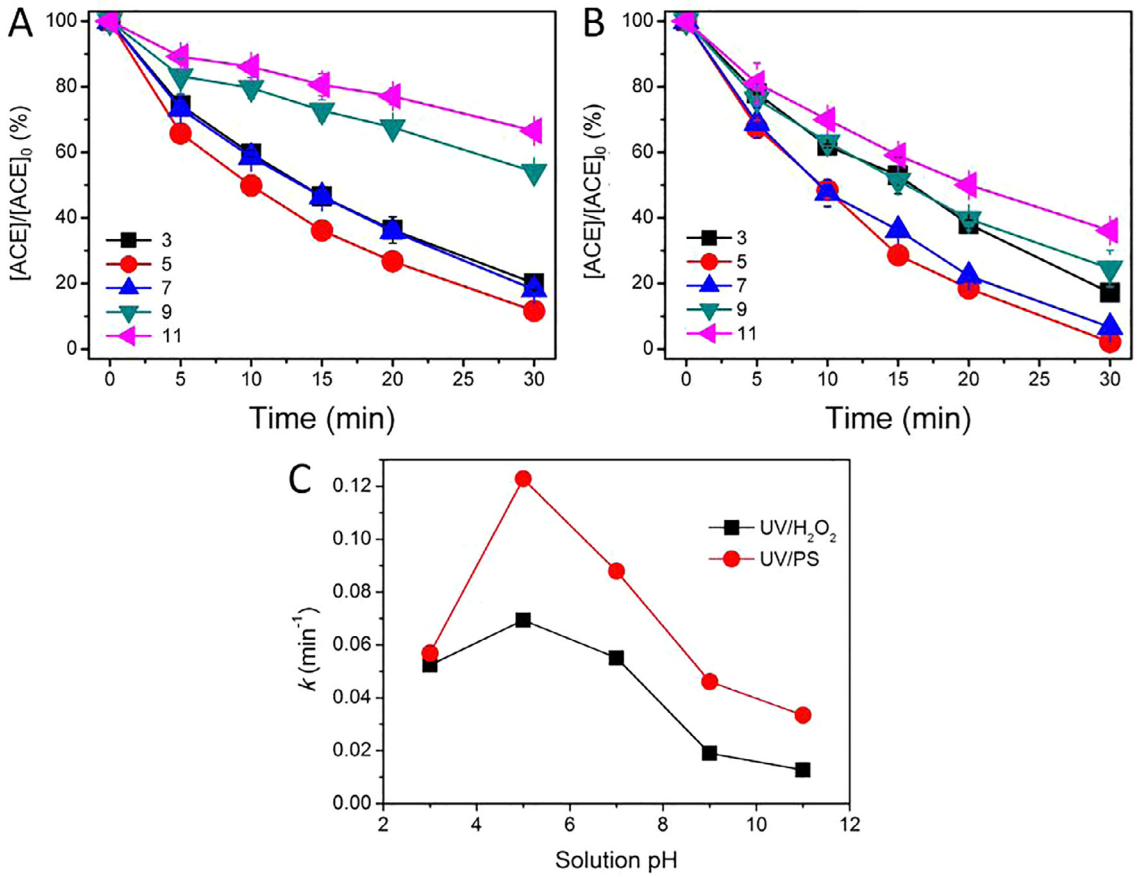

Fig. 3. The degradation of ACE in UV/H_2O_2 (A) and UV/PS (B) systems at different solution pHs. ([ACE] = 90 μM, [H_2O_2] = 11.8 mM, [$K_2S_2O_8$] = 1.5 mM, T = 25 °C).

from Nernst equation) [27]. In addition, the reaction between OH^- and HO· would be enhanced at basic conditions through Eq. (4) [30]. The generated O·$^-$ was less reactive with a redox potential of only 1.78 V. Noticeably, when the pH came to 11, the predominant form of H_2O_2 would be the hydroperoxide anion HO_2^- [47], which possessed a much higher UV_{254} absorption coefficient than H_2O_2 [48]. The much higher UV_{254} absorption coefficient of HO_2^- might significantly depress the decomposition of H_2O_2 to HO· under UV irradiation. Moreover, the HO_2^- exhibited a much higher reaction rate constant with HO· (Eq. (5), $k = 7.5 \times 10^9\ M^{-1}\ s^{-1}$ [49]) than with H_2O_2 ($k = 2.7 \times 10^7\ M^{-1}\ s^{-1}$ [30]), making it a strong scavenger towards HO·. Therefore, the reduction of the redox potential of HO· and the scavenging effects of OH^-/HO_2^- both accounted for the lower ACE degradation rate at higher pH value.

$$OH^- + HO^{\cdot} \rightarrow H_2O + O^{\cdot -} \quad (4)$$

$$HO_2^- + HO^{\cdot} \rightarrow OH^- + HO_2^{\cdot} \quad (5)$$

$$OH^- + SO_4^{\cdot -} \rightarrow HO^{\cdot} + SO_4^{2-} \quad pH = 11 \quad (6)$$

For the UV/PS process, a similar inhibition phenomenon was observed for the high pH conditions. This was because the HO· was massively generated through the reaction between $SO_4^{\cdot -}$ and OH^- (Eq. (6)) at high pH condition [24]. The generated HO· possessed slow rate constant (as demonstrated in Fig. 1). On the other hand, the $SO_4^{\cdot -}$ was the predominant radical species under the acidic condition [26].

Overall, the acidic and neutral conditions were favorable for the ACE degradation in UV based AOPs. This was also in consistent with a previous work that reported the photolysis of ACE was favorable in acidic ($k = 0.0119\ min^{-1}$ at pH = 4) and neutral conditions whilst depressed in basic condition ($k = 0.0061\ min^{-1}$ at pH = 9) [28].

3.4. Effect of aqueous matrix species

The inorganic anions and natural organic matters (NOM) ubiquitously occurred in natural water bodies usually participate in the degradation process during the field applications of the UV based AOPs and bring positive/negative effects on the removal performance. Therefore, chloride (Cl^-), bicarbonate (HCO_3^-), nitrate (NO_3^-), and humic acid (HA) were selected in this case to investigate their potential effects on the ACE degradation by UV/H_2O_2 and UV/PS processes.

It was reported that Cl^- could scavenge active radicals (HO· and $SO_4^{\cdot -}$) to form less reactive species ($ClOH^{\cdot -}$, Cl· and $Cl_2^{\cdot -}$) through Eqs. (7–10), leading to a decreased degradation efficiency [23,30]. Consequently, as shown in Fig. 4, the degradation process was clearly depressed in the both processes. Similarly, Zhang et al. [27] indicated that the presence of Cl^- reduced the degradation of azathioprine in both UV/H_2O_2 and UV/PS systems. Compared with UV/PS process, the negative effect of Cl^- on UV/H_2O_2 process was much more insignificant. This was probably attributed to that the few $ClOH^{\cdot -}$ could rapidly revert back to Cl^- and HO· under neutral condition (Eq. (11)) [23]. Moreover, the ratio of [Cl^-]/[Oxidant] was relatively low in UV/H_2O_2 system compared with that in UV/PS system, which also might be the plausible reason for the weak inhibition.

HCO_3^- could also react with HO· and $SO_4^{\cdot -}$ to produce $CO_3^{\cdot -}$, a less reactive species (Eqs. (12) and (13)). Thus, the inhibition of the degradation process was usually expected in the presence of HCO_3^-. However, quite interestingly, this was not the case in the present study. As shown in Fig. 4, HCO_3^- in the concentration of 5–15 mM brought negative effect on UV/PS process, whilst slightly promoted the ACE degradation by UV/H_2O_2 process. Liu et al. [44] also reported that the HCO_3^- promoted the degradation of oxytetracycline by UV/H_2O_2 and

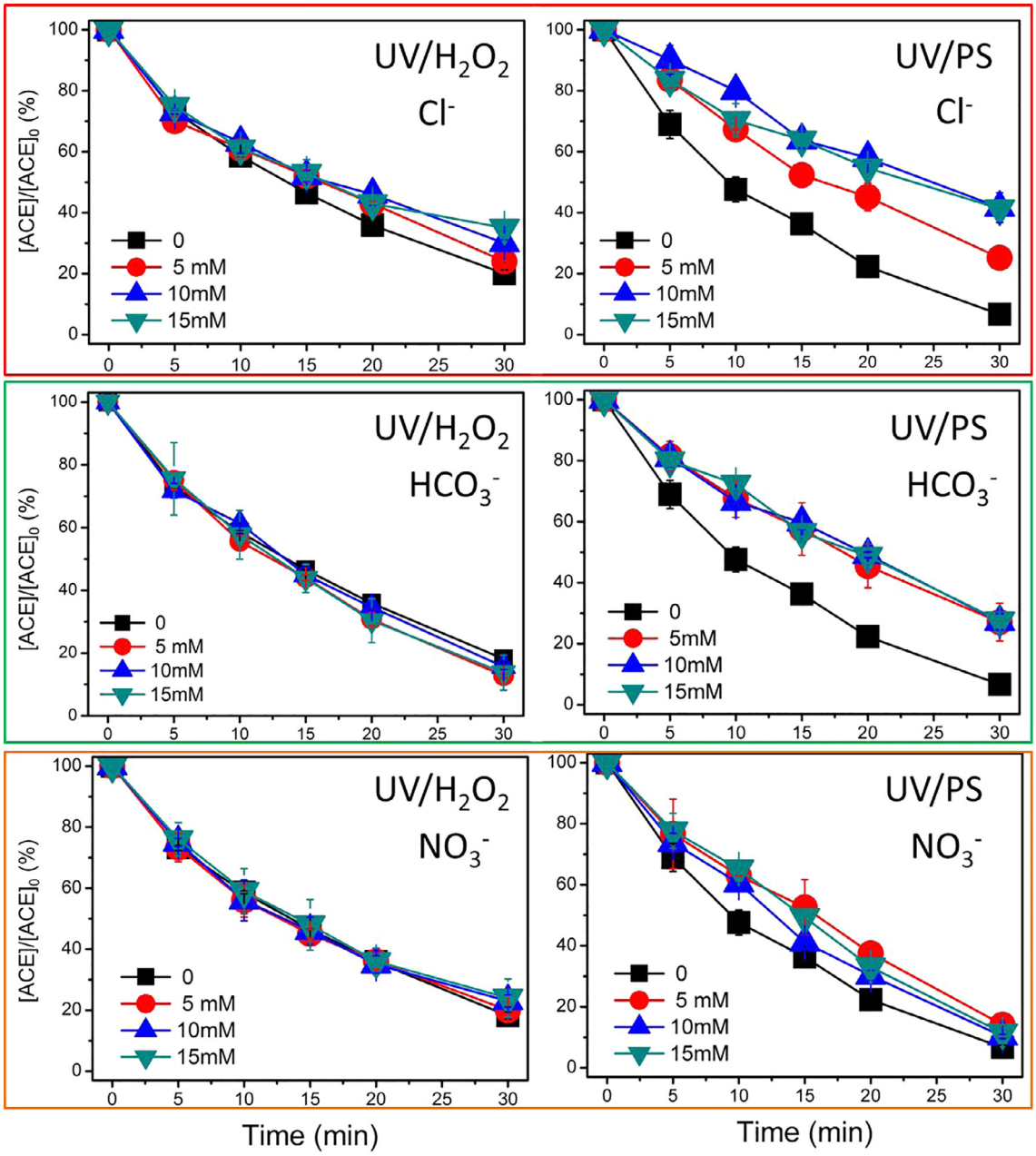

Fig. 4. Effects of Cl^-, HCO_3^-, and NO_3^- on the degradation of ACE in UV/H_2O_2 and UV/PS systems. ([ACE] = 90 μM, [H_2O_2] = 11.8 mM, [$K_2S_2O_8$] = 1.5 mM, pH = 7, T = 25 °C).

UV/PS processes. The adverse effects were probably dependent on the concentration of HCO_3^-. In contrast, NO_3^- did not give rise to an obvious positive/negative effects on the degradation processes. This was probably due to its slow reaction rates with radical species (Eq. (14)).

HA generally plays two important roles in the UV based AOPs, radical scavenger and UV absorption agent [50]. It was reported that the second-order rate constant of Suwannee River Humic Acid (SRHA) with $SO_4^{\cdot -}$ was $2.35 \times 10^7\ M^{-1}\ s^{-1}$ [51], which was much lower than that with HO·. Therefore, SRHA played a lower scavenging effect in UV/PS process than UV/H_2O_2 process. On the other hand, HA could also lead to a photosensitization process involving reactive oxygen species by absorbing UV radiation and enhance the degradation process. As shown in Fig. 5, the dose of HA clearly brought negative effects on the ACE degradation by UV/PS process. The similar phenomenon was well documented in previous works [25,50]. Noticeably, the degradation rate was significantly reduced to < 20% in the UV/PS process when the dose of HA was 15 mg L^{-1}, probably indicating its low efficiency in treating NOM-rich wastewater. On the contrary, the degradation process was slightly improved in the UV/H_2O_2 system with the low dose of HA (5 mg L^{-1}). Tan et al. [42] found that the low level of HA (2.5 mg L^{-1}) was beneficial (catalytic effect) while high level of HA was inhibitory (scavenging effect) for the degradation process. In this case, the dosage of HA (5–15 mg L^{-1}) was relatively low when comparing with that of H_2O_2. However, this dosage was higher in the UV/PS system because the concentration of $K_2S_2O_8$ was only 1.5 mM. This result clearly suggested that the effect of HA was also dependent on its concentration. In other words, the negative effects of HA could be crippled by increasing the dosage of chemical oxidants.

$$Cl^- + HO^{\cdot} \rightarrow ClOH^{\cdot -} \quad k = 4.3 \times 10^9\ M^{-1}s^{-1} \tag{7}$$

$$ClOH^{\cdot -} + H^+ \rightarrow Cl^{\cdot} + H_2O \quad k = 3.0 \times 10^{10}\ M^{-1}s^{-1} \tag{8}$$

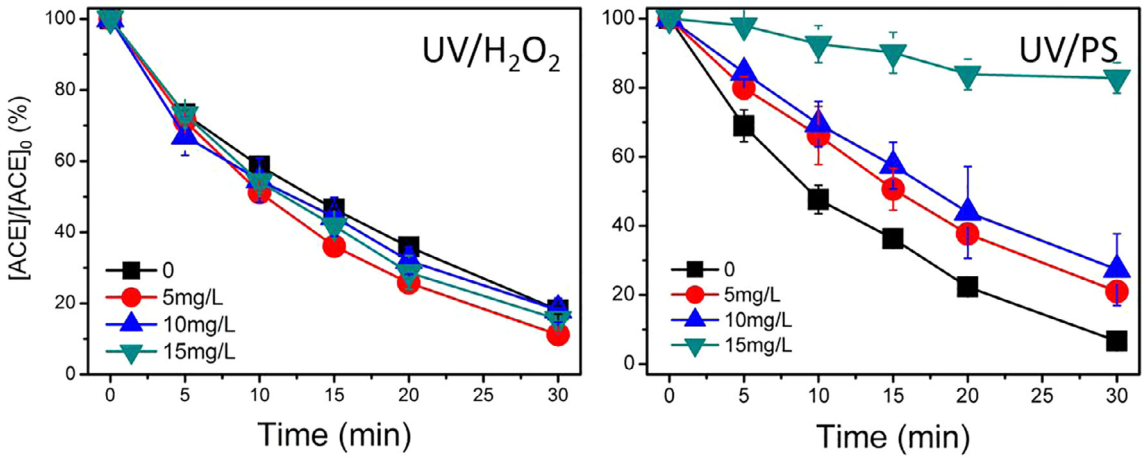

Fig. 5. Effect of HA on the degradation of ACE in UV/H_2O_2 and UV/PS systems. ([ACE] = 90 μM, [H_2O_2] = 11.8 mM, [$K_2S_2O_8$] = 1.5 mM, pH = 7, T = 25 °C).

$$ClOH^{\cdot} + Cl^- \rightarrow Cl_2^{\cdot -} + OH^- \quad k = 1.0 \times 10^5\ M^{-1}\ s^{-1} \tag{9}$$

$$Cl^- + SO_4^{\cdot -} \rightarrow Cl^{\cdot} + SO_4^{2-} \quad k = 3.1 \times 10^8\ M^{-1}\ s^{-1} \tag{10}$$

$$ClOH^{\cdot -} \rightarrow Cl^- + HO^{\cdot} \quad k = 6.0 \times 10^9\ M^{-1} s^{-1} \tag{11}$$

$$HCO_3^- + HO^{\cdot} \rightarrow CO_3^{\cdot -} + H_2O \quad k = 8.5 \times 10^6\ M^{-1}\ s^{-1} \tag{12}$$

$$HCO_3^- + SO_4^{\cdot -} \rightarrow CO_3^{\cdot -} + HSO_4^- \quad k = 9.1 \times 10^6\ M^{-1} s^{-1} \tag{13}$$

$$NO_3^- + SO_4^{\cdot -} \rightarrow NO_3^{\cdot} + SO_4^{2-} \quad k = 5 \times 10^4\ M^{-1} s^{-1} \tag{14}$$

3.5. Identification of radical species

The active radical species in the UV base AOPs were identified by using methanol and *tert*-butanol as radical scavengers. According to their distinct reactivity towards HO· and $SO_4^{\cdot -}$, their respective contributions to the ACE degradation were distinguished [23,24]. Specifically, the decrease of the degradation rate after adding *tert*-butanol was attributed to the contribution of HO·. Similarly, the decrease observed after adding methanol was attributed to the total contributions of HO· and $SO_4^{\cdot -}$.

As depicted in Fig. 6, only HO· contributed for the ACE degradation by UV/H_2O_2 process while both HO· and $SO_4^{\cdot -}$ contributed in UV/PS process. The occurrence of HO· in the UV/PS process was reasonable because the reaction between $SO_4^{\cdot -}$ and H_2O (Eq. (15)). Moreover, the main reactive radical species was HO· while $SO_4^{\cdot -}$ played a minor role during the degradation process in the UV/PS process. Similarly, the HO· made a non-negligible contribution during the degradation of β-lactam antibiotics in the UV/PS system [26].

$$SO_4^{\cdot -} + H_2O \rightarrow HO^{\cdot} + SO_4^{2-} + H^+ \quad k < 60\ M^{-1}\ s^{-1}\ (pH = 7) \tag{15}$$

3.6. TOC variation

The degree of mineralization during the ACE degradation process was respectively assessed and the results were given in Fig. 7. The complete mineralization usually takes a much longer time compared with the partly decomposition of organic compounds due to the generation of recalcitrant intermediates [50]. As shown, though the ACE could be completely removed within 1 h, the TOC removal rate was even lower than 40%. After 2 h's treatment, the TOC removal rate achieved 50% for the UV/PS process, while it was only 26.6% for the UV/H_2O_2 process. The results clearly revealed that a large part of ACE was transformed into intermediates rather than completely mineralized. Similarly, up to 50% of TOC was removed within 6 h though the ACE diminished in the first minute of the Fenton process [7]. The poor TOC reduction was extensively reported in the degradation processes of other organic compounds by UV based AOPs [26].

In addition, a remarkable difference between the two processes in terms of the TOC removal was also presented. The UV/PS process exhibited a much higher TOC removal efficiency than the UV/H_2O_2 process, which was in well agreement with the ACE elimination profiles (Fig. 1). Similar results had been reported in previous studies [27,52]. Considering the lower second-order rate constant between $SO_4^{\cdot -}$ and ACE and the minor contribution of $SO_4^{\cdot -}$, the higher TOC removal rate

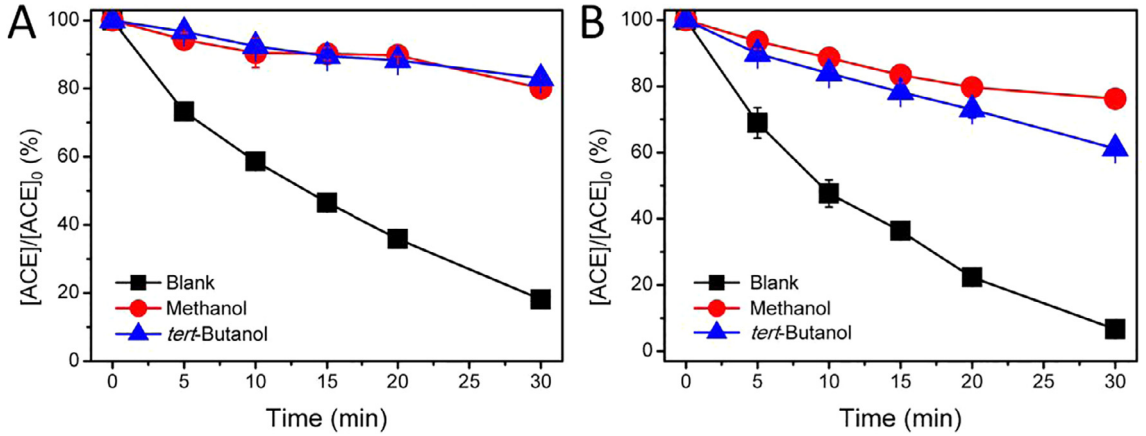

Fig. 6. Contributions of radical species during the degradation processes in UV/H_2O_2 (A) and UV/PS (B) systems. ([ACE] = 90 μM, [H_2O_2] = 11.8 mM, [$K_2S_2O_8$] = 1.5 mM, [Methanol] = [*tert*-Butanol] = 1 M, pH = 7, T = 25 °C).

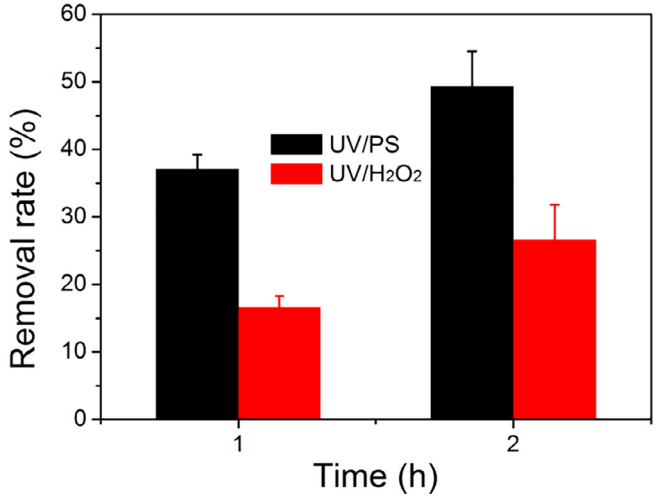

Fig. 7. The variations of TOC during the degradation process. ([ACE] = 90 μM, $[H_2O_2]$ = 11.8 mM, $[K_2S_2O_8]$ = 1.5 mM, pH = 7, T = 25 °C).

was probably attributed to the more generated HO· in UV/PS than in UV/H_2O_2 process.

3.7. Degradation products

Due to the distinct reaction mechanisms between free radicals and organic compounds [53], different products might be generated by UV/H_2O_2 and UV/PS processes [27,42]. The degradation product was directly related with the degree of mineralization (TOC removal efficiency) and toxicity of effluent. As shown in Fig. 7, the TOC removal efficiency was lower than 40% within 1 h while the ACE was absent, indicating the ACE was partly transformed into intermediates other than completely mineralized. Therefore, the ultimate degradation products were analyzed through HPLC-MS.

As shown in the HPLC spectra (Fig. 8), several peaks were clearly observed, indicating that the ACE was transformed into several intermediates. This was well agreed with the preceding TOC results. In addition, more products were identified in the UV/PS process, which was not strange because both HO· and $SO_4^{\cdot -}$ presented in UV/PS process while only HO· was detected in UV/H_2O_2 process (Fig. 7). The HO· non-selectively attacked the organic compounds mainly through hydrogen abstraction or electrophilic addition mechanism [48]. On the other hand, $SO_4^{\cdot -}$ was more likely to do that through the electron transfer reactions [30].

Table 2
The characteristics of the real waters.

Item	YR	TL	SE
COD_{Cr} (mg L^{-1})	< 5[a]	< 5[a]	429 ± 12.7
TOC (mg L^{-1})	1.644	3.315	139.4
TIC (mg L^{-1})	26.3	31.58	304.7
Salinity (g/L)	0.53	0.95	9.75
Cl^- (mg L^{-1})	19.35	20.47	16.8
NO_3^- (mg L^{-1})	1.63	0.15	1.58
pH	7.30	6.98	8.07

[a] The values are under the limitations of detection according to the standard detection method.

For the identification of the degradation intermediates, the mass spectra was recorded and given in Fig. 8C. The protonated ACE molecular possessed a charge-to-mass ratio (*m/z*) of 223.2. It was documented that the hydroxylated product (M − OH) was usually detected in the HO· and $SO_4^{\cdot -}$ induced degradation processes [27]. For example, the hydroxylated ACE (with *m/z* 239.0) was found in a previous study which investigated the degradation of ACE with Fenton process [54,55]. As in this case, the molecular ion peak with an *m/z* of 238.9 was detected, which was therefore assigned to the hydroxylated ACE (+16 Da). In addition, the intermediate with an *m/z* of 209.0 was also identified in the both oxidation processes. According to the previous study, the demethylation reaction usually occurred in the free radical induced oxidation process [27]. Therefore, this intermediate could be assigned to the demethylated derivative (−14 Da) [54,56].

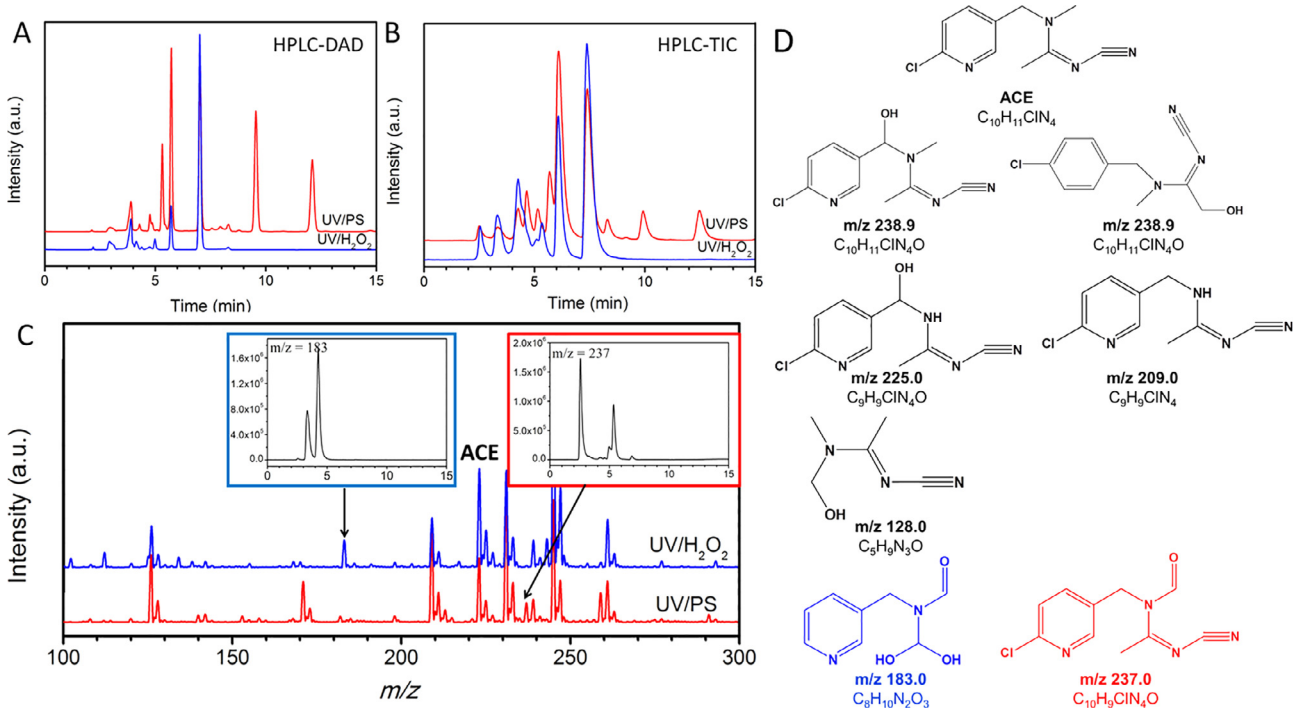

Fig. 8. HPLC (A: diode array detector (DAD) chromatogram, B: total ion chromatogram (TIC)), corresponding mass spectra (C), and proposed structure (D) of the ACE degradation products in UV/H_2O_2 and UV/PS systems. Inset of C shows the extracted ion chromatograms (EIC) of *m/z* 171, 183, and 259, respectively.

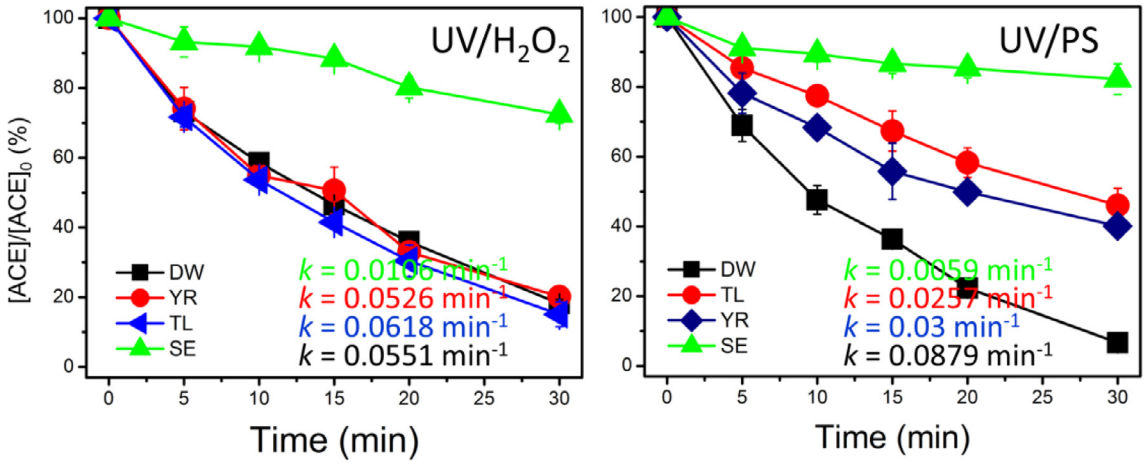

Fig. 9. Degradation of ACE by UV/H_2O_2 and UV/PS systems in different water matrices. ([ACE] = 90 μM, [H_2O_2] = 11.8 mM, [$K_2S_2O_8$] = 1.5 mM, pH = 7, T = 25 °C).

Noticeably, we also found some unique peaks in different oxidation processes. For example, the molecular ion peaks at *m/z* 171 (−52 Da), 237 (+14 Da), and 259 (+36 Da) were only observed in UV/PS process while absent in UV/H_2O_2 process. Among them, the structure of the product with *m/z* of 237 was proposed based on the previous study [54]. However, the structures of the other two products were still obscure and need to be further characterized in the future. Similarly, the molecular ion peak at *m/z* 183 (−40 Da) was only observed in the UV/H_2O_2 process. Sirtori et al. [54] proposed a non-chlorinated molecular ion ($C_8H_{10}N_2O_3$, *m/z* 183) during the degradation of ACE by Fenton process based on the four fragment ions (155, 137, 109, 68). According to the previously documented structures of the byproducts of ACE, the possible structures of the degradation intermediates detected in this study were proposed (Fig. 8D). Nevertheless, more evidences were needed to confirm the proposed structures.

3.8. Degradation of ACE in real waters

The feasibility of the UV based AOPs in degrading ACE from real waters (TL, YR, and SE) was evaluated in this study. The characteristics of the collected real waters were presented in Table 2.

Due to the occurrence of high level NOM and salinity, the degradation process was significantly inhibited in SE by both UV/H_2O_2 and UV/PS processes (Fig. 9). The degradation rate constants decreased from 0.0551 min^{-1} and 0.0879 min^{-1} to 0.0106 min^{-1} and 0.0059 min^{-1}, respectively. Noticeably, the UV/H_2O_2 process performed better stability than UV/PS, agreeing well with the results shown in Figs. 4 and 5. Moreover, probably ascribed to the extremely high concentration of TOC, the promotion effect brought by the HA in UV/H_2O_2 process (Fig. 5) disappeared. Large amounts of NOM would scavenge the reactive radical species and compete for the UV radiation, remarkably inhibiting the generation of radical species. The concentrations of inorganic anions were comparable among the three types of real waters. According to the preceding discussion, the relatively low concentrations (< < 5 mM) of Cl^- and NO_3^- in the real waters would not produce significant negative effects on the degradation process. Therefore, it was concluded that the NOM occurred in the real water played a vital role in the ACE degradation by UV based AOPs. Xiao et al. [50] compared the degradation of iodoacids from river water, treated water, and SE by UV/H_2O_2 and UV/PS processes, respectively. Similarly, they found the worst degradation rate in the SE no matter for the UV/H_2O_2 or UV/PS process. This result suggests that a pretreatment for the removal of NOM was necessary for the application of UV based AOPs in some real waters such as SE.

In addition, the degradation process was moderately decreased in TL and YR water compared with in DW for the UV/PS process. Probably due to the relatively low concentration of TOC, the degradation rate constant was higher in YR than in TL. On the other hand, the degradation of ACE in TL and YR was comparable with that in DW for the UV/H_2O_2 process. This was well agreed with the results in Fig. 5.

4. Conclusions

This paper evaluated the ACE degradation by UV/H_2O_2 and UV/PS processes. The combination of UV and chemical oxidants (H_2O_2 or PS) significantly improved the degradation of ACE. Specifically, UV/PS process showed better degradation performance than UV/H_2O_2 at the same dosage of PS and H_2O_2 probably due to the higher radical yield in UV/PS process. Moreover, the degradation process was highly dependent on the solution pH. Inorganic anions ubiquitously existed in natural waters exhibited negative effects on the degradation process due to the scavenging effect except NO_3^-. Humic acid significantly inhibited the degradation process due to the scavenging effect and competition of radiation. Only HO· contributed to the degradation process by UV/H_2O_2 while both HO· and $SO_4^{\cdot -}$ were responsible for the degradation of ACE in UV/PS process. The corresponding second-order rate constants of ACE with HO· and $SO_4^{\cdot -}$ were determined to be 7.59×10^8 and $3.68 \times 10^8\ M^{-1}s^{-1}$, respectively. Different degradation products were detected in the two processes. Eventually, the degradation process was inhibited to some extent in real waters, especially in the secondary effluent of wastewater.

Acknowledgement

This work is financially supported by the National Natural Science Foundation of China (No. 51608274) and the Fundamental Research Funds for the Central Universities (KYZ 201619, KJQN 201749).

Appendix A. Supplementary data

Supplementary data associated with this article can be found, in the online version, at http://dx.doi.org/10.1016/j.cej.2018.06.107.

References

[1] M. Mateu-Sanchez, M. Moreno, F. Javier Arrebola, José Luis M. Vidal, Analysis of acetamiprid in vegetables using gas chromatography-tandem mass spectrometry, Anal. Sci. 19 (2003) 701–704.
[2] S.K. Pramanik, J. Bhattacharyya, S. Dutta, P.K. Dey, A. Bhattacharyya, Persistence of acetamiprid in/on mustard (Brassica juncea L.), B Environ. Contam. Tox. 76 (2006) 356–360.
[3] S. Gupta, V.T. Gajbhiye, Persistence of acetamiprid in soil, B. Environ. Contam. Tox.

78 (2007) 349–352.
[4] D. Sanyal, D. Chakma, S. Alam, Persistence of a neonicotinoid insecticide, acetamiprid on Chili (Capsicum annum L.), B. Environ. Contam. Tox. 81 (2008) 365–368.
[5] United States Environmental Protection Agency, Code of federal regulations (CFR), Part 180, Washington, DC, Washington, DC, 2005.
[6] K.N.N. Henshushitsu, Noyaku Toroku Horyu Kijun handbook, Tokyo, Japan, 1998.
[7] E.E. Mitsika, C. Christophoridis, K. Fytianos, Fenton and Fenton-like oxidation of pesticide acetamiprid in water samples: kinetic study of the degradation and optimization using response surface methodology, Chemosphere 93 (2013) 1818–1825.
[8] A. Bernabeu, R.F. Vercher, L. Santos-Juanes, P.J. Simón, C. Lardín, M.A. Martínez, J.A. Vicente, R. González, C. Llosá, A. Arques, A.M. Amat, Solar photocatalysis as a tertiary treatment to remove emerging pollutants from wastewater treatment plant effluents, Catal. Today 161 (2011) 235–240.
[9] J.A. Sánchez Peréz, I. Carra, C. Sirtori, A. Agüera, B. Esteban, Fate of thiabendazole through the treatment of a simulated agro-food industrial effluent by combined MBR/Fenton processes at μg/L scale, Water Res. 51 (2014) 55–63.
[10] Scientific opinion on the developmental neurotoxicity potential of acetamiprid and imidacloprid, EFSA J., 11 (2013), 3471.
[11] J.T. Marfo, K. Fujioka, Y. Ikenaka, S.M.M. Nakayama, H. Mizukawa, Y. Aoyama, M. Ishizuka, K. Taira, Relationship between urinary N-desmethyl-acetamiprid and typical symptoms including neurological findings: a prevalence case-control study, PLOS One 10 (2015) e0142172.
[12] A. Cruz-Alcalde, C. Sans, S. Esplugas, Priority pesticides abatement by advanced water technologies: the case of acetamiprid removal by ozonation, Sci. Total Environ. 599–600 (2017) 1454–1461.
[13] N.D. Banić, D.V. Šojić, J.B. Krstić, B.F. Abramović, Photodegradation of neonicotinoid active ingredients and their commercial formulations in water by different advanced oxidation processes, Water Air Soil Pollut. 225 (2014) 1954.
[14] H. Yang, X. Wang, J. Zheng, G. Wang, Q. Hong, S. Li, R. Li, J. Jiang, Biodegradation of acetamiprid by Pigmentiphaga sp. D-2 and the degradation pathway, Int. Biodeter. Biodegr. 85 (2013) 95–102.
[15] H. Tang, J. Li, H. Hu, P. Xu, A newly isolated strain of Stenotrophomonas sp. hydrolyzes acetamiprid, a synthetic insecticide, Process Biochem. 47 (2012) 1820–1825.
[16] A. Adak, K.P. Mangalgiri, J. Lee, L. Blaney, UV irradiation and UV-H_2O_2 advanced oxidation of the roxarsone and nitarsone organoarsenicals, Water Res. 70 (2015) 74–85.
[17] B.A. Wols, C.H.M. Hofman-Caris, D.J.H. Harmsen, E.F. Beerendonk, Degradation of 40 selected pharmaceuticals by UV/H_2O_2, Water Res. 47 (2013) 5876–5888.
[18] B.F. Abramović, N.D. Banić, D.V. Šojić, Degradation of thiacloprid in aqueous solution by UV and UV/H_2O_2 treatments, Chemosphere 81 (2010) 114–119.
[19] Y. Cao, H. Tan, T. Shi, T. Tang, J. Li, Preparation of Ag-doped TiO_2 nanoparticles for photocatalytic degradation of acetamiprid in water, J. Chem. Technol. Biotechnol. 83 (2008) 546–552.
[20] A. Khan, M.M. Haque, N.A. Mir, M. Muneer, C. Boxall, Heterogeneous photocatalysed degradation of an insecticide derivative acetamiprid in aqueous suspensions of semiconductor, Desalination 261 (2010) 169–174.
[21] I. Carra, J.A. Sánchez Pérez, S. Malato, O. Autin, B. Jefferson, P. Jarvis, Application of high intensity UVC-LED for the removal of acetamiprid with the photo-Fenton process, Chem. Eng. J. 264 (2015) 690–696.
[22] I. Carra, J.A. Sánchez Pérez, S. Malato, O. Autin, B. Jefferson, P. Jarvis, Performance of different advanced oxidation processes for tertiary wastewater treatment to remove the pesticide acetamiprid, J. Chem. Technol. Biot. 91 (2016) 72–81.
[23] P. Neta, R.E. Huie, A.B. Ross, Rate constants for reactions of inorganic radicals in aqueous solution, J. Phys. Chem. Ref. Data 17 (1988) 1027–1284.
[24] P. Neta, V. Madhavan, H. Zemel, R.W. Fessenden, Rate constants and mechanism of reaction of sulfate radical anion with aromatic compounds, J. Am. Chem. Soc. 99 (1977) 163–164.
[25] Q. Wang, Y. Shao, N. Gao, W. Chu, X. Shen, X. Lu, J. Chen, Y. Zhu, Degradation kinetics and mechanism of 2,4-Di-tert-butylphenol with UV/persulfate, Chem. Eng. J. 304 (2016) 201–208.
[26] X. He, S.P. Mezyk, I. Michael, D. Fatta-Kassinos, D.D. Dionysiou, Degradation kinetics and mechanism of β-lactam antibiotics by the activation of H_2O_2 and $Na_2S_2O_8$ under UV-254 nm irradiation, J. Hazard. Mater. 279 (2014) 375–383.
[27] Y. Zhang, J. Zhang, Y. Xiao, V.W.C. Chang, T.-T. Lim, Kinetic and mechanistic investigation of azathioprine degradation in water by UV, UV/H_2O_2 and UV/persulfate, Chem. Eng. J. 302 (2016) 526–534.
[28] X. Guohong, L. Guoguang, S. Dezhi, Z. Liqing, Kinetics of acetamiprid photolysis in solution, B. Environ. Contam. Tox. 82 (2009) 129–132.
[29] N. Daneshvar, M.A. Behnajady, M.K.A. Mohammadi, M.S.S. Dorraji, UV/H_2O_2 treatment of Rhodamine B in aqueous solution: influence of operational parameters and kinetic modeling, Desalination 230 (2008) 16–26.
[30] G.V. Buxton, C.L. Greenstock, W.P. Helman, A.B. Ross, Critical review of rate constants for reactions of hydrated electrons, hydrogen atoms and hydroxyl radicals (·OH/·O^-) in aqueous solution, J. Phys. Chem. Ref. Data 17 (1988) 513–886.
[31] R. Zhang, Y. Yang, C.-H. Huang, L. Zhao, P. Sun, Kinetics and modeling of sulfonamide antibiotic degradation in wastewater and human urine by UV/H_2O_2 and UV/PDS, Water Res. 103 (2016) 283–292.
[32] The State Environmental Protection Administration, Water and Wastewater Monitoring and Analysis Method, fourth ed., China Environmental Science Press, Beijing, 2002 (in Chinese).
[33] F.J. Beltrán, M. González, J.F. González, Industrial wastewater advanced oxidation. Part 1. UV radiation in the presence and absence of hydrogen peroxide, Water Res. 31 (1997) 2405–2414.
[34] V.J. Pereira, H.S. Weinberg, K.G. Linden, P.C. Singer, UV degradation kinetics and modeling of pharmaceutical compounds in laboratory grade and surface water via direct and indirect photolysis at 254 nm, Environ. Sci. Technol. 41 (2007) 1682–1688.
[35] I. Kim, H. Tanaka, Photodegradation characteristics of PPCPs in water with UV treatment, Environ. Int. 35 (2009) 793–802.
[36] Y. Guan, J. Ma, X. Li, J. Fang, L. Chen, Influence of pH on the formation of sulfate and hydroxyl radicals in the UV/peroxymonosulfate system, Environ. Sci. Technol. 45 (2011) 9308–9314.
[37] W. Chu, Y.R. Wang, H.F. Leung, Synergy of sulfate and hydroxyl radicals in UV/$S_2O_8^{2-}$/H_2O_2 oxidation of iodinated X-ray contrast medium iopromide, Chem. Eng. J. 178 (2011) 154–160.
[38] J. Deng, Y. Shao, N. Gao, S. Xia, C. Tan, S. Zhou, X. Hu, Degradation of the antiepileptic drug carbamazepine upon different UV-based advanced oxidation processes in water, Chem. Eng. J. 222 (2013) 150–158.
[39] S. Yang, P. Wang, X. Yang, L. Shan, W. Zhang, X. Shao, R. Niu, Degradation efficiencies of azo dye Acid Orange 7 by the interaction of heat, UV and anions with common oxidants: persulfate, peroxymonosulfate and hydrogen peroxide, J. Hazard. Mater. 179 (2010) 552–558.
[40] G.P. Anipsitakis, D.D. Dionysiou, Transition metal/UV-based advanced oxidation technologies for water decontamination, Appl. Catal. B 54 (2004) 155–163.
[41] G. Mark, M.N. Schuchmann, H.-P. Schuchmann, C. von Sonntag, The photolysis of potassium peroxodisulphate in aqueous solution in the presence of tert-butanol: a simple actinometer for 254 nm radiation, J. Photochem. Photobiol. A 55 (1990) 157–168.
[42] C. Tan, N. Gao, Y. Deng, Y. Zhang, M. Sui, J. Deng, S. Zhou, Degradation of antipyrine by UV, UV/H_2O_2 and UV/PS, J. Hazard. Mater. 260 (2013) 1008–1016.
[43] N. Gao, Y. Deng, D. Zhao, Ametryn degradation in the ultraviolet (UV) irradiation/hydrogen peroxide (H_2O_2) treatment, J. Hazard. Mater. 164 (2009) 640–645.
[44] Y. Liu, X. He, Y. Fu, D.D. Dionysiou, Kinetics and mechanism investigation on the destruction of oxytetracycline by UV-254 nm activation of persulfate, J. Hazard. Mater. 305 (2016) 229–239.
[45] D. Ding, C. Liu, Y. Ji, Q. Yang, L. Chen, C. Jiang, T. Cai, Mechanism insight of degradation of norfloxacin by magnetite nanoparticles activated persulfate: identification of radicals and degradation pathway, Chem. Eng. J. 308 (2017) 330–339.
[46] C. Zhao, M. Pelaez, X. Duan, H. Deng, K. O'Shea, D. Fatta-Kassinos, D.D. Dionysiou, Role of pH on photolytic and photocatalytic degradation of antibiotic oxytetracycline in aqueous solution under visible/solar light: kinetics and mechanism studies, Appl. Catal. B 134–135 (2013) 83–92.
[47] C.N. Sawyer, P.L. McCarty, G.F. Parkin, Chemistry for Environmental Engineering and Science, McGraw Hill Higher Education, 2003.
[48] J.H. Baxendale, J.A. Wilson, The photolysis of hydrogen peroxide at high light intensities, Trans. Faraday Soc. 53 (1957) 344–356.
[49] H. Christensen, K. Sehested, H. Corfitzen, Reactions of hydroxyl radicals with hydrogen peroxide at ambient and elevated temperatures, J. Phys. Chem. 86 (1982) 1588–1590.
[50] Y. Xiao, L. Zhang, J. Yue, R.D. Webster, T.-T. Lim, Kinetic modeling and energy efficiency of UV/H_2O_2 treatment of iodinated trihalomethanes, Water Res. 75 (2015) 259–269.
[51] P. Xie, J. Ma, W. Liu, J. Zou, S. Yue, X. Li, M.R. Wiesner, J. Fang, Removal of 2-MIB and geosmin using UV/persulfate: contributions of hydroxyl and sulfate radicals, Water Res. 69 (2015) 223–233.
[52] J. Criquet, N.K.V. Leitner, Degradation of acetic acid with sulfate radical generated by persulfate ions photolysis, Chemosphere 77 (2009) 194–200.
[53] F. Minisci, A. Citterio, C. Giordano, Electron-transfer processes: peroxydisulfate, a useful and versatile reagent in organic chemistry, Acc. Chem. Res. 16 (1983) 27–32.
[54] C. Sirtori, A. Agüera, I. Carra, J.A. Sanchéz Pérez, Application of liquid chromatography quadrupole time-of-flight mass spectrometry to the identification of acetamiprid transformation products generated under oxidative processes in different water matrices, Anal. Bioanal. Chem. 406 (2014) 2549–2558.
[55] I. Carra, C. Sirtori, L. Ponce-Robles, J.A. Sánchez Pérez, S. Malato, A. Agüera, Degradation and monitoring of acetamiprid, thiabendazole and their transformation products in an agro-food industry effluent during solar photo-Fenton treatment in a raceway pond reactor, Chemosphere 130 (2015) 73–81.
[56] L. Polgár, J.F. García-Reyes, P. Fodor, A. Gyepes, M. Dernovics, L. Abrankó, B. Gilbert-López, A. Molina-Díaz, Retrospective screening of relevant pesticide metabolites in food using liquid chromatography high resolution mass spectrometry and accurate-mass databases of parent molecules and diagnostic fragment ions, J. Chromatogr. A 1249 (2012) 83–91.